Received 7 April 2017; revised 12 June 2017; accepted 17 June 2017. Date of publication 11 July 2017;
date of current version 23 August 2017. The review of this paper was arranged by Editor C.-M. Zetterling.

Digital Object Identifier 10.1109/JEDS.2017.2721916

Selective Fabrication of SiC/Si Heterojunction Diodes by Local Laser Annealing Process for Microwave Circuit Applications

AMANPREET KAUR (Member, IEEE), TIMOTHY HOGAN (Senior Member, IEEE), AND PREMJEET CHAHAL (Member, IEEE)

Department of Electrical and Computer Engineering, Michigan State University, East Lansing, MI 48824-1226, USA

CORRESPONDING AUTHOR: AMANPREET KAUR (e-mail: kaurama1@msu.edu)

This work was supported by the DARPA YFA Program under Grant N66001-12-1-4238.

ABSTRACT This paper presents the RF characterization of SiC/Si heterojunction diodes fabricated using a novel localized laser process. Selective growth of SiC on Si is carried out by utilizing excimer laser-based annealing in the presence of carbon source. Use of ambient conditions (atmospheric pressure and room temperature) during growth makes this process simple and low cost. The Si wafer is first coated with carbon rich film and then locally annealed using high power laser which causes dissociation of solid carbon sources and a simultaneous melting of the silicon leading to the growth of SiC. The Raman spectrum shows peaks for acoustical and optical phonon modes for β-SiC between 940 and 980 cm^{-1}. The fabricated diodes show high breakdown voltage (>200 V) and low leakage current density of 3-5 $\mu A/cm^2$ (−5 V). Experimental results for the dc characteristics, microwave rectification and frequency multiplication are presented. The measured results show good RF rectification (e.g., 21 V/W at 3 GHz) up to 6 GHz using a large diode (70×70 μm^2). The diodes also work well as frequency doublers over a wide frequency range of 2–6 GHz. The diode area can be scaled down to design circuits operating at higher frequencies.

INDEX TERMS CMOS integrated circuits, frequency multiplication, heterojunction diodes, high power, laser, microwave rectification, silicon carbide, silicon.

I. INTRODUCTION

Affordable high power microwave devices are desired for applications such as base station transceiver and automotive collision avoidance systems [1], [2]. High frequency solid state devices are limited by transit time and thus smaller size devices are needed to achieve high cut-off frequency. The high power and high frequency circuits require devices based on semiconductor materials with both large breakdown voltage and high electron velocity. Wide bandgap materials like gallium nitride (GaN) and silicon carbide (SiC) are of particular interest as they can handle high power densities unlike conventional semiconductors [3], [4]. GaN and SiC based devices grown on Silicon (Si) substrate are foreseen as one of the best candidates for next generation systems that require seamless integration of RF and digital circuits in close proximity to each other. A variety of microwave devices based on GaN and SiC have been demonstrated in the past including Schottky barrier diodes, metal semiconductor field effect transistors (MESFETs), heterojunction bipolar transistors (HBTs), high electron mobility transistors (HEMTs), and impact ionization avalanche transit-time diodes (IMPATT) [5]–[7].

SiC has also gained interest for power applications due to its higher thermal conductivity in comparison to GaN, and it can also theoretically withstand higher power densities. Out of the various existing polytypes of SiC, 3C-SiC is of interest as it can be grown directly on Si and also has the highest electron mobility. Tremendous effort has been directed towards direct growth and integration of high quality SiC and GaN devices on Si substrate for monolithic microwave integrated circuits (MMICs). Next generation of circuits require CMOS circuitry for data conditioning and signal processing along

with high power RF devices. The most common integration techniques studied are hybrid integration and hetero-epitaxy. Hybrid integration approaches, such as wire bonding and flip chip, provide a short term solution. However, it has many limitations in terms of interconnect losses and die placement/alignment issues, and integration density. A more attractive approach is the hetero-epitaxy of different semiconductors onto Si substrate. The biggest challenge in direct growth of compound semiconductors (CS) on Si is lattice mismatch and coefficient of thermal expansion (CTE) mismatch. CTE mismatch is a bigger problem as the growth is usually carried out at temperatures above 1000 °C causing accumulation of thermal mismatch at the junction. In recent years, different approaches have been used to solve this challenge such as buffer layer engineering to suppress crack formation [8], [9], low temperature molecular beam epitaxy (MBE) [10], and plasma enhanced chemical vapor deposition (PECVD) [11].

Another attractive approach is to grow the materials locally or selectively on Si substrate. It allows optimizing the performance of circuits through strategic placement of CS based microwave devices and CMOS devices on a common silicon substrate. The selective area growth can also help in reducing misfit dislocation density in lattice mismatched systems by reducing dislocation interaction and multiplication [12]. As the growth area is limited to few mm^2, the quality of heterogeneously grown CS can be better optimized. Recently, local epitaxy of InP-based HBT structures were reported on lithography defined lattice engineered Si substrate (wafer with growth windows) using MBE at 650°C [13]. However, these techniques require complex epi-layer engineering, unique silicon substrate wafer for local epitaxial growth and heating of the whole substrate. So, there is a need for alternate low cost growth techniques for integration of high power microwave circuits along with CMOS devices while limiting exposure of existing circuits on Si to high temperature.

Recently, growth of SiC on Si has been demonstrated using furnace annealing (FA) and rapid thermal annealing (RTA) of pre deposited carbon (C60) films on Si. The annealing process causes diffusion of carbon into Si [14], [15]. Although RTA requires much lower temperature than the conventional CVD or FA because of enhanced SiC crystallization at high heating rates but it still requires heating of the whole substrate. To overcome this challenge, Kaur *et al.* [16] recently demonstrated selective area growth of SiC /Si heterojunction (HJ) diodes using a high power KrF (nanosecond) excimer laser. The laser based technique uses focused high power laser beam to locally anneal the pre deposited carbon source on a Si substrate. Laser based process is a perfect solution as it provides localized heating and it has been used as an alternative to classical FA or RTA for various applications such as doping of crystalline Si and recrystallization of amorphous Si film [17], [18]. Therefore, it is expected that laser can be used to grow SiC on Si by annealing the pre-deposited carbon film.

Kaur *et al.* [16] demonstrated the use of this new laser based process in the fabrication of photo-diode. This paper presents experimental demonstration of laser processed SiC/Si HJ diodes for high frequency applications, to the best of our knowledge, for the first time. The use of laser as a heat source for growth process offers several advantages: (a) spatial resolution and control, (b) limited damage to the substrate and neighboring circuits, (c) possibility of cleaner film due to small area heating and, (d) rapid (non-equilibrium) heating and cooling rate. The details of the laser based process, material characterization, DC and RF characterization of SiC/Si HJ diodes are presented in the follow on sections.

II. DEVICE FABRICATION

The SiC/Si diodes were fabricated on two types of wafers (p-type) with different carrier concentrations and thickness. The diodes made on the low doped wafer ($N_a = 4.3\times10^{14}$ cm^{-3}, thickness = 250μm) are referred to as diode A and diodes made on the high doped wafer (N_a $\sim3\times10^{15}cm^{-3}$, the thickness of 150$\mu$m) are referred to as diode B.

The wafers were first cleaned with acetone and isopropyl alcohol in an ultrasonic bath for 5 min each, followed by a 5 min rinse in deionized (DI) water. The wafers were then cleaned by buffered hydrofluoric acid (HF) solution to remove native oxide followed by a DI water rinse. This was followed by spin coating of a thin layer of PMMA (∼400 nm), and baking for 90 sec at 180 °C. The wafer was then placed on an XYZ manipulator in open air environment and at room temperature. The sample was then irradiated with a high power KrF excimer laser (λ = 248 nm, pulse duration ∼25 ns). The excimer laser beam was directed onto the substrate through an optical path which homogenizes and shapes the intensity profile to achieve uniform illumination across the desired focal area. Confinement (localization) of energy is achieved by controlling the laser spatial profile by focusing the beam through optics, and beam shaping through homogenizers, apertures and refractive elements [19]. The repetition rate of the pulsed laser is fixed at 1 Hz and the number of pulses radiating the substrate is controlled using an external trigger unit.

Laser irradiation with very high power dissociates solid carbon sources and melts silicon leading to the growth of SiC. Use of lasers with smaller wavelength (248 nm) allows local modification of surface properties without altering the properties of the bulk region. The growth of SiC on Si is carried out through localized heating while holding the substrate under ambient conditions (in air at atmospheric pressure and at room temperature). The irradiated area of Si undergoes melting and re-crystallization in a very short period of time. The laser beam simultaneously decomposes PMMA and melts the Si surface. The PMMA provides a solid carbon source for SiC synthesis. The key mechanism for laser processing of semiconductors with high power lasers is photo-thermal (pyrolytic), where the absorbed laser energy

is directly transformed into heat. High power laser with fluences above the threshold of melting of material can lead to much higher solubility than in the solid phase which results in rapid material homogenization [20]. The average area of SiC region is 350 x 500 μm^2 which is dictated by the focusing optics.

To realize RF circuits with working frequencies in the GHz range, much smaller devices than this area are needed. Thus, further processing is carried out to reduce the device area and to deposit the contacts. The steps to fabricate small area diodes and to make contacts to Si and SiC are depicted in Figure 1(c-f). The SiC/Si diodes are also coupled into the coplanar waveguide (CPW) feed network structures for on-wafer probing and high frequency characterization. First, a thin layer of Ni (200 nm) is deposited by e-beam deposition followed by deposition of 200 nm of Al (Figure 1(b)). The bottom Ni is used as the Ohmic contact to SiC while Al is used here as a hard mask for etching SiC using SF_6/O_2 based reactive ion etching (RIE). The metals were patterned and etched to open a window for etching SiC. Al was etched using H_3PO_4: HAc: HNO_3:H_2O (16:1:1:2) and Ni was etched using $FeCl_3$.

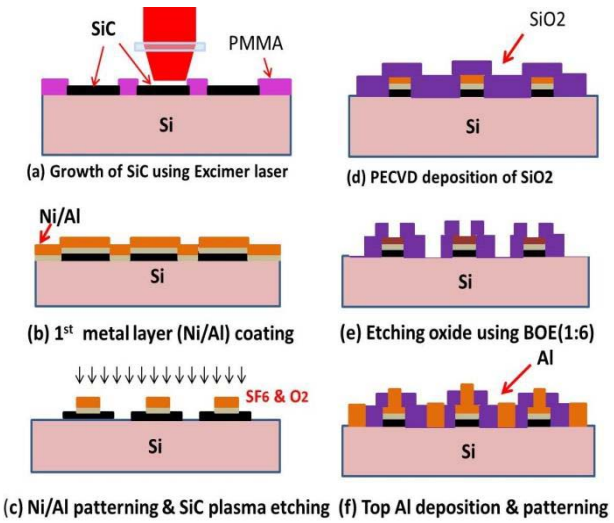

FIGURE 1. Fabrication steps for RF SiC/Si diodes.

After patterning of the first layer, SiC was etched using SF_6 and O_2 plasma, Figure 1(c), using a power of 200 W, plasma time of 3 min, SF_6 /O_2 flow of 20/5 sccm. The diode junction area achieved after etching SiC was $\sim$ 70 x 70 μm^2. After etching the SiC, 300nm of SiO_2 was deposited using a PECVD process as shown in Figure 1(d). The oxide was grown to passivate the surface after etching SiC. The oxide was patterned to open a window to the Si, Figure 1(e). The 2nd metal layer (Al) was then deposited as an Ohmic contact to the Si side of the diode. In the final step, the 2nd metal was patterned, Figure 1(f). The Ohmic contacts on both the SiC and Si were annealed at 450 °C for 5 min to improve the contact formation and reduce the series resistance. This step is important in order to improve the high frequency performance of the diodes.

The fabricated CPW structure is shown in Figure 2. The ground pad of CPW directly contacts the Si substrate, and the signal pad contacts the SiC layer. The SiC/Si diode characteristics were measured between the ground and signal pads. Several SiC/Si devices were formed using a different number of laser pulses. The best devices are formed by 2 pulses, similar to the work presented by Kaur *et al.* [16]. Here, in this paper, the DC and RF characterization of devices fabricated from SiC formed using 2 laser pulses is presented on two different wafers having different doping concentrations.

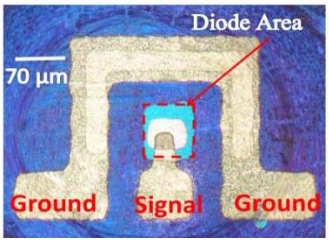

FIGURE 2. Optical micrograph of fabricated CPW structure with SiC/Si diode.

The Raman spectra for the device fabricated using 2 laser pulses is shown in Figure 3. The Raman measurement was carried out in backscattering geometry using a 532 nm laser. The peak at 521 cm^{-1} is from the silicon substrate and the peaks between 940cm^{-1} and 980cm^{-1} are due to acoustical and optical phonon modes of β-SiC.

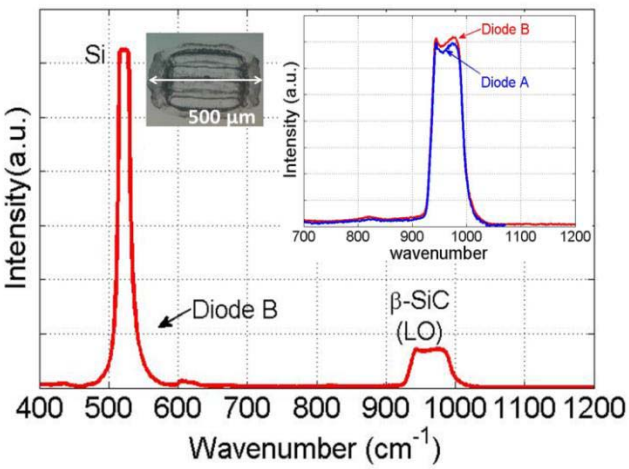

FIGURE 3. Measured Raman spectra of SiC/Si for device with 2 laser pulses, the optical image of the SiC area (inset).

The peak broadening is due to the damping of phonon modes by short range ordering of SiC crystallites [21]. The usual forbidden transverse optic (TO) mode around 796 cm^{-1} is not observed here; however, the LO mode peaks match with work presented in [22] and [23]. The absence of TO mode also suggests the absence of stacking faults, stress, and dislocations at the interface [24]. The inset of

Figure 3 shows the Raman spectra measurements of materials of Diode A (on lightly doped wafer) and Diode B (on higher doped wafer). The inset also shows optical image of SiC/Si structure fabricated using 2 laser pulses.

III. EXPERIMENTAL RESULTS

A. CURRENT – VOLTAGE CHARACTERISTICS

All the device measurements presented in this paper were carried at room temperature, in open air environment, and under dark conditions using a Keithley 2400 source meter. The measurements are shown for the best performing diodes made from 2 laser pulse processed structure (optimum power transfer). Figure 4 and 5 shows the measured current density-voltage (J-V) characteristics of the large area (500 x 350 μm^2) SiC/Si diode over a large voltage range for diode type A and diode type B, respectively. Both diodes show a high reverse breakdown voltage of >200V with very small leakage current. The breakdown voltage for the diodes made with 2 pulses is much higher than 200V but limited by measurement set-up. Diode type A shows leakage current density of ~3$\mu A/cm^2$ (-5V), while diode type B shows the slightly higher current density of ~5$\mu A/cm^2$ (-5V) as expected due to higher doping of Si. Both the diodes show barrier height of ~0.4 eV as shown in the inset of Figure 4 & 5. The type B diodes show higher forward current as expected due to a higher doping level of wafer.

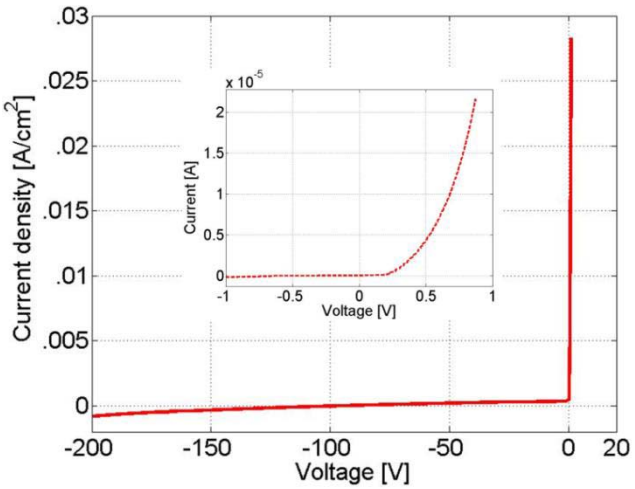

FIGURE 4. Measured J-V characteristics of SiC/Si based diodes (Type A) fabricated on a low doped wafer. The inset shows curve fit to the diode equation.

The measured leakage current is lower than previously reported SiC/Si diodes fabricated using standard techniques such as CVD and sputtering [25]–[27]. The CVD grown SiC contains a large number of extended defects due to the lattice and CTE mismatch which results in high leakage current. Here, the small leakage current indicates fewer defects at the interface. This is largely due to the localized growth of SiC which helps in reducing misfit dislocation [27]. It can also be concluded from the J-V measurements that the conductivity of the SiC layer is n-type which is due to unintentional doping of SiC with nitrogen which has very low binding energy of 15–20 meV. This suggests that nitrogen from the ambient is incorporated in the film during laser process.

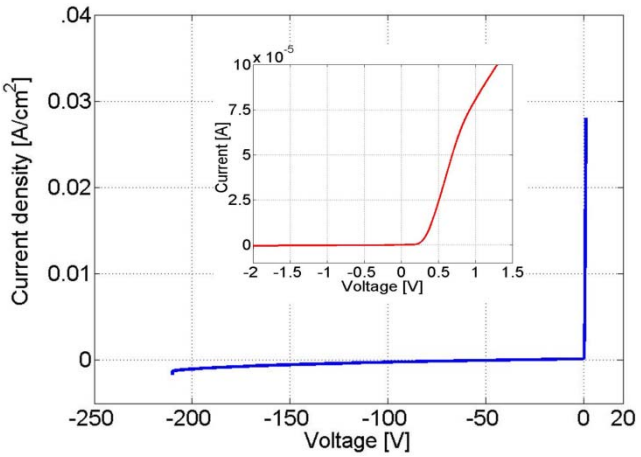

FIGURE 5. Measured J-V characteristics of SiC/Si based diodes (Type B) fabricated on the wafer with high doping. The inset shows curve fit to the diode equation.

B. SIC/SI DIODE BASED MICROWAVE RECTIFICATION

Microwave or millimeter wave detectors are needed for applications such as wireless power transmission, concealed weapon detection, medical imaging, and energy recycling [28]. For high power rectification, devices based on wide-bandgap semiconductors are required. Here, the performance of SiC/Si HJ diodes fabricated using a laser process was investigated for microwave detection. The RF to DC rectification characteristics of the diode was measured by directly injecting RF power to the diode placed in a 50-Ω CPW structure using GSG coplanar RF probes, and all the measurements were carried out at room temperature. For the measurement setup, (RF+DC) signal was applied to the device through a CPW probe, T-Bias and via a directional coupler (HP87300B). The directional coupler was used to acquire incident and reflected signal from the device. The reflected/incident signal was measured using a spectrum analyzer. High frequency losses in the setup were also measured in order to estimate the actual power delivered to the device. Figures 6 & 7 show the rectified current as a function of frequency for diodes type A and B, respectively, and at a fixed bias of ~0.35 V (strongest non-linearity point) and RF power of ~0 dBm. To measure the rectified or detected current the I-V characteristics were measured with RF on and off and change in the current was extracted. The results clearly show that the rectified current decrease as a function of frequency due to impedance mismatch.

The inset of Figure 6 & 7 shows the measured rectified current as a function of applied DC bias for diode type A (1 and 2 GHz) and diode type B (5 and 6 GHz) at fixed incident power of ~0 dBm. For both of the diodes the highest measured rectified voltage is near the bias voltage of ~0.35V, which is close to the strongest non-linearity point of the

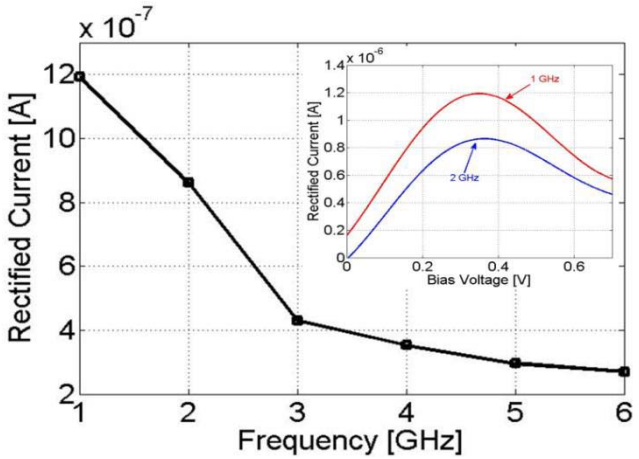

FIGURE 6. **Rectified current vs frequency for SiC/Si RF diodes for Type A diode at a fixed bias of ~ 0.35 V and RF power of ~ 0 dBm. The inset shows rectified current as a function of DC bias ~ 0 dBm input RF power.**

diode. Type B diode exhibited better properties than type A diode, producing a much higher rectified current which is due to higher doping level. For example, type B diode showed rectified current of 35 μA at 2 GHz while in comparison to 0.86 μA for type A diode. In addition, the rectified current remained above ~ 1 μA over the entire measured frequency range (2-7 GHz) for diode B.

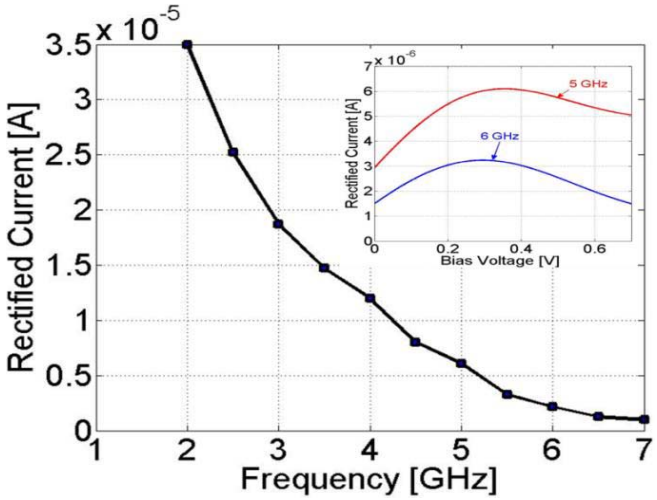

FIGURE 7. **Rectified current vs frequency for SiC/Si RF diodes for Type B diode at a fixed bias of ~ 0.35 V and RF power of ~ 0 dBm. The inset shows rectified current as a function of DC bias ~ 0 dBm input RF power.**

The measured result shows that the diode can act as a rectifier up to 6 GHz. The higher frequency performance of the device is limited by transit time which is related to the size of the diode and can further be improved by reducing the area of the diode. The maximum RF power applied to the diode was limited by the source, but it is expected that higher detected current can be achieved at higher power levels without break down. The diodes were measured multiple times (>10) to make sure they can withstand cycling of high power levels and similar results were achieved every time. Also, it was noted that stable DC output can obtained with continues RF illumination over a long time (>15min.) with no change in device performance.

On-wafer *S*-parameter measurements of several diodes placed in 50-Ω CPW feed structures were also carried out using the Network Analyzer (Agilent N5227A) up to 10 GHz at an input power level of -10 dBm. The *S*-parameter data was fitted to the diode equivalent model shown in Figure 8. The model consists of series resistance R_s, junction resistance R_d, and junction capacitance C_d which can be used to estimate voltage sensitivity (β_v) or current sensitivity (β_i) of the diode using the equations (1) and (2) [29]. Here, γ is curvature coefficient, Γ is mismatch losses, and 1- Γ^2 in equation (1) accounts for absorbed power. The curvature coefficient γ is the measurement of the nonlinearity of the diode current–voltage (I–V) characteristic and is given by the ratio of the second derivative of the diode I–V characteristics to its 1st derivative, in most of the case, $\gamma = q/nk_BT$. Where k_B is the Boltzmann Constant, T is the temperature, q is the electron charge and n is the ideality factor.

$$\beta_v = \beta_i(R_s + R_d) = \frac{\gamma\,(R_d + R_s)\,(1 - \Gamma 2)}{2(1 + R_s/R_d)^2(1 + (f/f_{ci})^2)} \quad (1)$$

$$f_{ci} = \frac{(1 + R_s/R_d)^{1/2}}{2\pi C_d (R_s R_d)^{1/2}} \quad (2)$$

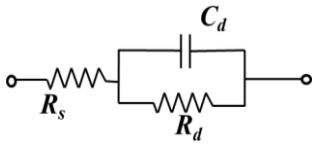

FIGURE 8. **Equivalent model of a diode.**

From the measured S-parameters, the extracted value of R_s, R_d and C_d are found to be 140 Ω, 700 Ω and 2800 fF, respectively. Using these values and γ of 14 for diode B, the predicted voltage sensitivity is 21, 7.74, 5.384 V/W at 3, 5 and 6 GHz, respectively. The voltage and current sensitivity are related to each other as shown in Equation (1) and can be used to calculate rectified current ($P_{in}\beta_i$). Figure 9 shows measured and calculated rectified current and a good match is obtained over the entire input power range. It can be verified from the slope of measured current in Figure 9 that the rectified voltage or current response changes linearly with input power over a wide power range (-18 dBm to 0 dBm) at the measured frequencies. In other words, it follows the square law detection. Discrepancy between the calculated and measured values is due to error in the measurement of power (~10%).

The diodes presented here show the rectification voltage sensitivity comparable to some of the previously reported GaN and SiC based diodes, see Table 1. The equivalent model of these diodes (R_d and C_j) was scaled with respect to area to compare with the measured value of the diode of this paper, 4900 μm^2. These results clearly show that

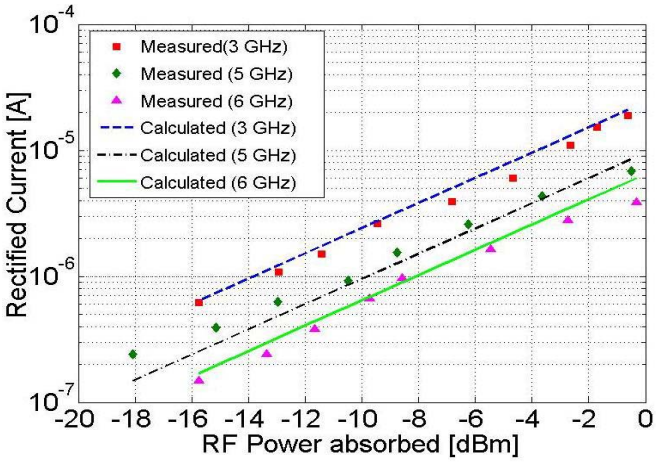

FIGURE 9. Measured rectified current at fixed bias (0.35 V) versus input power for SiC/Si RF diodes diode at 3, 5 and 6 GHz for type B diode.

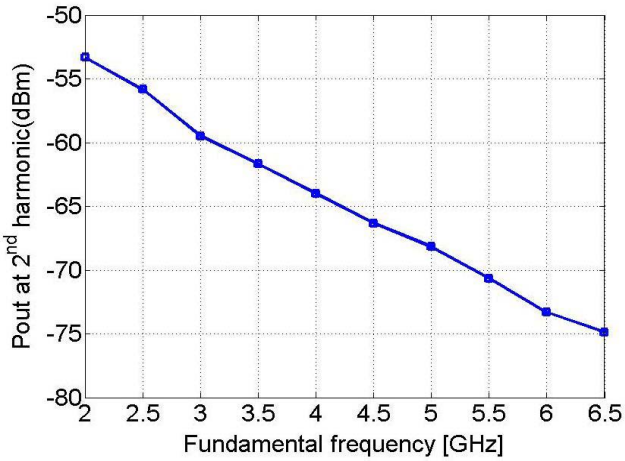

FIGURE 10. Measured output power of 2nd harmonic versus fundamental frequency of a SiC/Si (type B) diode at an input power of approximately -13 dBm.

the SiC/Si diodes can be used in the design of microwave circuits and have similar performance as reported in literature for different wide band gap devices. The diode performance can be further improved by lowering the series resistance and junction capacitance. In future lower series resistance can be achieved by annealing of the contacts which can be performed by laser itself to keep the heat localized to the growth region. To achieve lower capacitance, diodes with the smaller area can be used.

TABLE 1. Comparison of rectified voltage sensitivity for SiC/Si HJ diode of this paper to representative diodes presented in literature.

Type	Rs (Ω)	R_d (Ω)	Cj (fF)	F GHz	Sensitivity V/W	Ref
GaN SD	26	0.5	4410	3	6.9	[30]
SiC SD	2.5	7.5	7200	3	41	[31]
SiC/Si HJ	134	700	2800	3	21	This work

C. SIC/SI DIODE BASED FREQUENCY DOUBLER

Frequency multipliers are often used in a variety of applications such as frequency synthesizers, transceivers and future 60 GHz broadband wireless systems and automotive radar [32]. Frequency multiplication using SiC and GaN based diodes has been demonstrated in past [6], [7], [33]. There is great interest in developing low-cost frequency multipliers for compact, single-chip transceivers using Si-based technologies. However, for power applications hybrids SiC and GaN-based multipliers are still prominent. Here applicability of SiC/Si HJ diode for frequency multiplication circuits is reported. For the experimental set-up, the RF signal from a signal generator was supplied to the diode through a directional coupler (HP87300B) and output power at harmonics was measured using a spectrum analyzer. Figure 10 shows the output power of the second harmonic for a type B diode for fundamental frequencies in the range of 2 – 6.5 GHz at an input power level of -3 dBm.

The diode shows an output power -53 dBm for 2 x f_{in} = 4 GHz, and the highest measured output power remains above -72 dBm for frequencies up to 2 x f_{in} = 12 GHz. Considering the large size (70 x 70 μm^2), the device provides good performance in the GHz frequency range. The conversion efficiency of the diode decreases at higher frequencies due to transit time loss and impedance mismatch. Device size can be decreased to enhance performance at higher frequencies. Figure 11 shows the output power of the 2nd harmonic as a function of input power at fundamental frequencies of 2 and 4 GHz. The output power increases linearly with input power; over the entire input power range, demonstrating stable operation of the diode. Higher input power levels were not used due to the presence of higher harmonics from the source. The diode is expected to show a continuous linear response even at high power levels as it is clear from rectification results where high RF power was successfully applied without any breakdown.

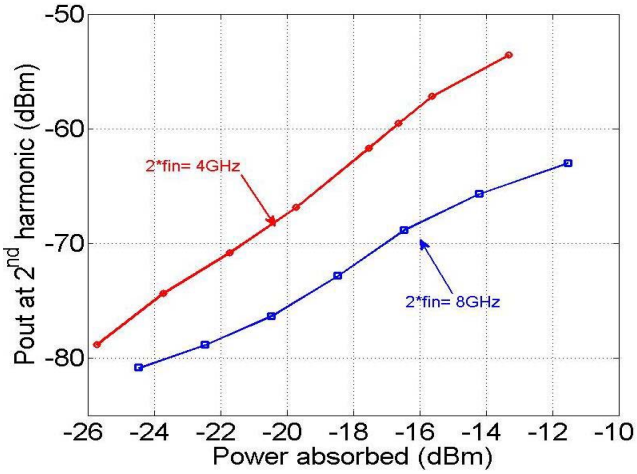

FIGURE 11. Measured output power of 2nd harmonic for SiC/Si at fundamental frequencies of 2 and 4 GHz.

The measured results of the 2nd harmonic are extrapolated for higher input levels in order to compare the conversion loss with previously reported frequency multipliers based on wide bandgap materials, see Table 2. Conversion loss (CL) of 14 dB is obtained at input RF power of 10 dBm which is comparable to results reported in literature. Conversion loss can be reduced by decreasing the series resistance of the diode. It can further be reduced by employing impedance matching technique and using a bandpass filter to avoid harmonics from the source.

TABLE 2. Summary of measured frequency multiplication in this paper and values reported in the literature (CL = conversion loss).

Diode type	Area (μm^2)	P_{in} (dBm)	Freq (GHz)	CL (dB)	Ref
GaN SD	19.6	23	33	22	[6]
GaN SD	30	21.76	100	8.22	[33]
SiC SD	490	19	1.56	7	[7]
SiC/Si HJ	4900	10	2	14*	This work

*extrapolated from measured results

IV. CONCLUSION

SiC/Si heterojunction diodes are fabricated using a novel laser processing technique using a high power KrF (nanosecond) excimer laser to locally grow SiC on Si substrate. The completed diodes are tested for RF and microwave circuit applications. This laser fabrication process has potential in developing low cost, high power microwave diodes by enabling direct localized growth on Si substrates. This process can potentially serve as an alternative to conventional techniques for heterogeneous integration of SiC devices on a CMOS wafer. This process offers limited damage to the substrate and neighboring circuits as the energy is absorbed near the surface region (modifying the surface chemistry) due to strong UV absorption by Si.

The small area diodes for RF characterization were successfully fabricated, showing strong non-linear I-V characteristics with low leakage current. In particular, diodes with contact area of 70 μm × 70 μm are fabricated and characterized. Diodes fabricated using a highly doped wafer showed higher forward current and provided better RF characteristics due to lower series resistance. The best performing diode showed microwave rectification sensitivity of 21V/W (at 3 GHz). The envisioned applications of these rectifiers are in high power wireless power transfer. In addition to rectification, SiC/Si HJ diodes were also tested as frequency doublers. Diodes on higher doped wafers show frequency multiplication in the 4-12 GHz range. These results clearly attest to the possibility of high-performance SiC-based electronic devices on low-cost large area Si substrates. This technology can potentially reduce cost and improve performance of systems for commercial applications such as high-speed communications, automotive collision avoidance, compact power converters and radar systems.

REFERENCES

[1] A. Osseiran *et al.*, "Scenarios for 5G mobile and wireless communications: The vision of the METIS project," *IEEE Commun. Mag.*, vol. 52, no. 5, pp. 26–35, May 2014.
[2] F. H. Raab *et al.*, "Power amplifiers and transmitters for RF and microwave," *IEEE Trans. Microw. Theory Techn.*, vol. 50, no. 3, pp. 814–826, Mar. 2002.
[3] U. K. Mishra, L. Shen, T. E. Kazior, and Y.-F. Wu, "GaN-based RF power devices and amplifiers," *Proc. IEEE*, vol. 96, no. 2, pp. 287–305, Feb. 2008.
[4] R. S. Pengelly, S. M. Wood, J. W. Milligan, S. T. Sheppard, and W. L. Pribble, "A review of GaN on SiC high electron-mobility power transistors and MMICs," *IEEE Trans. Microw. Theory Techn.*, vol. 60, no. 6, pp. 1764–1783, Jun. 2012.
[5] Z. H. Feng *et al.*, "High-frequency multiplier based on GaN planar Schottky barrier diodes," in *Proc. IEEE MTT-S Int. Microw. Workshop Series Adv. Mater. Process. RF THz Appl. (IMWS-AMP)*, Chengdu, China, 2016, pp. 1–3.
[6] R. N. Simons and P. G. Neudeck, "Intermodulation-distortion performance of silicon-carbide Schottky-barrier RF mixer diodes," *IEEE Trans. Microw. Theory Techn.*, vol. 51, no. 2, pp. 669–672, Feb. 2003.
[7] R. S. Pengelly, S. M. Wood, J. W. Milligan, S. T. Sheppard, and W. L. Pribble, "A review of GaN on SiC high electron-mobility power transistors and MMICs," *IEEE Trans. Microw. Theory Techn.*, vol. 60, no. 6, pp. 1764–1783, Jun. 2012.
[8] H. Sun, A. R. Alt, H. Benedickter, and C. R. Bolognesi, "High-performance 0.1-μm gate AlGaN/GaN HEMTs on silicon with low-noise figure at 20 GHz," *IEEE Electron Device Lett.*, vol. 30, no. 2, pp. 107–109, Feb. 2009.
[9] F. Medjdoub *et al.*, "First demonstration of high-power GaN-on-silicon transistors at 40 GHz," *IEEE Electron Device Lett.*, vol. 33, no. 8, pp. 1168–1170, Aug. 2012.
[10] T. Hatayama, Y. Tarui, T. Fuyuki, and H. Matsunami, "Low-temperature heteroepitaxial growth of cubic SiC on Si using hydrocarbon radicals by gas source molecular beam epitaxy," *J. Cryst. Growth*, vol. 150, pp. 934–938, May 1995.
[11] Q. Cheng, S. Xu, J. Long, and K. Ostrikov, "Low−temperature PECVD of nanodevice−grade nc−3C−SiC," *Chem. Vapor Deposition*, vol. 13, no. 10, pp. 561–566, 2007.
[12] E. A. Fitzgerald, "The effect of substrate growth area on misfit and threading dislocation densities in mismatched heterostructures," *J. Vac. Sci. Technol. B, Nanotechnol. Microelectron. Mater. Process. Meas. Phenomena*, vol. 7, no. 4, pp. 782–788, 1989.
[13] T. E. Kazior *et al.*, "A high performance differential amplifier through the direct monolithic integration of InP HBTs and Si CMOS on silicon substrates," in *Proc. IEEE MTT-S Int. Microw. Symp. Dig. (MTT)*, Boston, MA, USA, 2009, pp. 1113–1116.
[14] C.-P. Cheng, T.-W. Pi, C.-P. Ouyang, and J.-F. Wen, "SiC formation by C60 molecules as a precursor: A synchrotron-radiation photoemission study of the carbonization process," *J. Vac. Sci. Technol. A, Vac. Surfaces Films*, vol. 24, no. 1, p. 70, 2006.
[15] B. H. Wu, C. K. Chung, and C. C. Peng, "Rapid thermal annealing enhanced crystalline SiC particles at lower formation temperature," in *Proc. 3rd IEEE Int. Conf. Nano/Micro Eng. Mol. Syst. (NEMS)*, Sanya, China, 2008, pp. 1181–1184.
[16] A. Kaur, P. Chahal, and T. Hogan, "Selective fabrication of SiC/Si diodes by excimer laser under ambient conditions," *IEEE Electron Device Lett.*, vol. 37, no. 2, pp. 142–145, Feb. 2016.
[17] P. M. Smith, P. G. Carey, and T. W. Sigmon, "Excimer laser crystallization and doping of silicon films on plastic substrates," *Appl. Phys. Lett.*, vol. 70, no. 3, pp. 342–344, 1997.
[18] R. Delmdahl and B. Fechner, "Large-area microprocessing with excimer lasers," *Appl. Phys. A*, vol. 101, no. 2, pp. 283–286, 2010.
[19] M. S. Brown and C. B. Arnold, "Fundamentals of laser-material interaction and application to multiscale surface modification," in *Laser Precision Microfabrication*. Heidelberg, Germany: Springer, 2010, pp. 91–120.
[20] S. Zhang, Y. Ren, and G. Lüpke, "Ultrashort laser pulse beam shaping," *Appl. Opt.*, vol. 42, no. 4, pp. 715–718, 2003.
[21] J. K. Seo, Y.-H. Joung, Y. Park, and W. S. Choi, "Substrate temperature effect on the SiC passivation layer synthesized by an RF magnetron sputtering method," *Thin Solid Films*, vol. 519, no. 20, pp. 6654–6657, Aug. 2011.

[22] Z. C. Feng, A. J. Mascarenhas, W. J. Choyke, and J. A. Powell, "Raman scattering studies of chemical−vapor−deposited cubic SiC films of (100) Si," *J. Appl. Phys.*, vol. 64, no. 6, pp. 3176–3186, 1988.
[23] J. Wasyluk *et al.*, "Raman investigation of different polytypes in SiC thin films grown by solid-gas phase epitaxy on Si (111) and 6H-SiC substrates," in *Materials Science Forum*. 2010, pp. 359–362.
[24] J. Zhu, S. Liu, and J. Liang, "Raman study on residual strains in thin 3C-SiC epitaxial layers grown on Si (001)," *Thin Solid Films*, vol. 368, no. 2, pp. 307–311, 2000.
[25] P. H. Yih, J. P. Li, and A. J. Steckl, "SiC/Si heterojunction diodes fabricated by self-selective and by blanket rapid thermal chemical vapor deposition," *IEEE Trans. Electron Devices*, vol. 41, no. 3, pp. 281–287, Mar. 1994.
[26] S. Kerdiles, A. Berthelot, R. Rizk, and L. Pichon, "Fabrication and properties of low-temperature ($\leq 600^\circ$ C) processed n-type nanocrystalline SiC/p-type crystalline Si heterojunction diodes," *Appl. Phys. Lett.*, vol. 80, no. 20, pp. 3772–3774, 2002.
[27] H. Colder, R. Rizk, L. Pichon, and O. Bonnaud, "Low-temperature processing and properties of nanocrystalline-SiC/crystalline Si heterojunction devices," *Solid-State Electron.*, vol. 50, no. 2, pp. 209–213, 2006.
[28] J. A. Hagerty, F. B. Helmbrecht, W. H. McCalpin, R. Zane, and Z. B. Popović, "Recycling ambient microwave energy with broadband rectenna arrays," *IEEE Trans. Microw. Theory Techn.*, vol. 52, no. 3, pp. 1014–1024, Mar. 2004.
[29] P. Chahal, F. Morris, and G. Frazier, "Zero bias resonant tunnel Schottky contact diode for wide-band direct detection," *IEEE Electron Device Lett.*, vol. 26, no. 12, pp. 894–896, Dec. 2005.
[30] K. Fukui *et al.*, "T-shaped anode GaN Schottky barrier diode for microwave power rectification," in *Proc. IEEE MTT-S Int. Microw. Workshop Series Innov. Wireless Power Transm. Technol. Syst. Appl.*, Kyoto, Japan, 2012, pp. 195–198.
[31] J. Eriksson, N. Rorsman, and H. Zirath, "4H-silicon carbide Schottky barrier diodes for microwave applications," *IEEE Trans. Microw. Theory Techn.*, vol. 51, no. 3, pp. 796–804, Mar. 2003.
[32] T. Baras and A. F. Jacob, "K-band frequency synthesizer with subharmonic signal generation and LTCC frequency tripler," in *Proc. Microw. Integr. Circuit Conf. (EuMICEur)*, Amsterdam, The Netherlands, 2008, pp. 466–469.
[33] J. V. Siles and J. Grajal, "Capabilities of GaN Schottky multipliers for LO power generation at millimeter-wave bands," in *Proc. 19th Int. Symp. Space Terahertz Technol.*, 2008, pp. 504–507.

AMANPREET KAUR (M'16) received the bachelor's degree from Punjab Technical University, India, in 2005, the master's degree from the PEC University of Technology, India, in 2007, and the Ph.D. degree in electrical engineering from Michigan State University, in 2016. She is currently a Research Associate with the Department of Electrical and Computer Engineering, Terahertz System Laboratory, Michigan State University. Her areas of interest include nanomaterials-based RF circuits on flex, radio frequency identification-based sensing, bio sensors, novel anti-counterfeit technologies, and smart packaging. She was a Lecturer with the Department of ECE, Chandigarh Engineering College, India, from 2007 to 2010. During the Ph.D., she explored novel nanomaterials and thin film-based technologies for microwave circuits on flex, fabrication of SiC/Si diodes using a novel low-cost laser process, and wireless chemical/bio sensors. She is currently developing a multilevel anti-counterfeit authentication technology for pharmaceutical drugs and food supply chain.

TIMOTHY (TIM) HOGAN received the B.S. degree in electrical engineering from Michigan Technological University, in 1988 and the Ph.D. degree from the Electrical Engineering and Computer Science Department, Northwestern University, in 1996. He spent two years as a Post-Doctoral Fellow with the Physics Department, University of Houston, and joined Michigan State University, in 1998. He has established a charge transport characterization and pulsed laser deposition laboratory. He has over 140 papers in print, six books/book chapters, and three patents. His research interests are in the development of electronic materials and devices. Recent efforts have focused on diamond electronics, thermoelectric materials and waste heat recovery devices, nanowire growth, and surface enhanced Raman spectroscopy. He was a recipient of an NSF CAREER Award, the MSU Withrow Award for Distinguished Scholarship, the Teacher Scholar Award, and the Withrow Award for Teaching Excellence. He has gained experience in computer controlled, temperature dependent transport measurements including: ac and dc electrical conductivity, thermoelectric power, thermal conductivity, mutual inductance, Hall effect, and impedance spectroscopy.

PREMJEET (PREM) CHAHAL (M'03) received the B.S. and M.S. degrees in electrical engineering from Iowa State University, Ames and the Ph.D. degree in electrical engineering from the Georgia Institute of Technology, Atlanta, in 1999. He was a Senior Researcher with Raytheon, Dallas, TX, USA, from 1999 to 2006 and Abbott Laboratories, Abbott Park, IL, USA, from 2006 to 2008. He developed many new technologies for sensing, devices, packaging, and components with Abbott Laboratories and Raytheon. He joined as a Faculty Member with Michigan State University, East Lansing, in 2009, and since 2015 holds the position of an Associate Professor. His research interests are in THz technology, millimeter-wave electronics, RF-based sensors, RF MEMS, RF-optical devices, and microwave and millimeter wave systems packaging. He was a recipient of the 2012 DARPA Young Faculty Award and the 2016 Withrow Teaching Excellence Award, and he holds eight U.S. patents.